For submission to *Quaternary Research*

January 9, 2003

QUANTIFYING EROSION AND DEPOSITION PROCESSES ON A COMPLEX, DISTURBED DESERT PIEDMONT, FT. IRWIN, CALIFORNIA

Kyle K. Nichols* Paul R. Bierman
School of Natural Resources and Department of Geology, University of Vermont, Burlington, Vermont 05405

Martha C. Eppes
Department of Geography and Earth Science, University of North Carolina Charlotte, Charlotte, North Carolina 28223

Marc Caffee**, Robert Finkel
Center for Accelerator Mass Spectrometry, Lawrence Livermore National Laboratory, Livermore, California 94405

Jennifer Larsen
Department of Geology, University of Vermont, Burlington, Vermont 05405

Now at:
*Department of Geosciences, Skidmore College, 815 N. Broadway, Saratoga Springs, New York 12866
email: knichols@skidmore.edu
phone: 518.580.5194
fax: 518.580.5199
** PRIME Laboratory, Purdue University, West Lafayette Indiana 47907

ABSTRACT

We measured ^{10}Be and ^{26}Al in 29 samples of sediment to estimate histories and process rates on the complex and heavily disturbed East Range Road piedmont, northern Mojave Desert. The upland basin erosion rates are low, 13 ± 3 mm kyr^{-1}, suggesting that upland basins supply comparatively little sediment to the piedmont. A large volume of sediment, which is now eroding, was deposited proximal to the uplands ~ 76,000 yrs ago. Deposition histories of the distal piedmont suggest three stable periods over the last 70,000 yrs. Long-term average sediment velocities range from 8 cm y^{-1} to 23 cm yr^{-1} from the uplands to 6 km down piedmont.

Sediment velocities down the Army disturbed East Range Road piedmont are similar to ^{10}Be estimated sediment velocities down three other undisturbed piedmonts in the Mojave Desert. Such similarity suggests that neither piedmont morphology nor human disturbance affect average, long-term rates of piedmont sediment transport. The approach we have taken provides baseline data with which to compare to contemporary sediment transport rates in order to understand better the degree to which human impact affects desert piedmonts.

INTRODUCTION

Long, low gradient surfaces (termed *piedmonts*) that extend away from desert mountains or uplands are common in the Mojave Desert and elsewhere (Thomas, 1997). Piedmonts, because they have a low-gradient and are accessible, are rapidly being developed to accommodate increasing population in the southwest United States (O'Hara, 1997). Human impact, mostly off-road vehicular disturbance, has been quantified over small areas and short time-scales (Iverson, 1980; Iverson *et al*., 1981; Nichols and Bierman, 2001; Persico *et al*., 2001; in review; Prose, 1985). However, the impact of human activities on large-scale, long-term

piedmont process rates is not known. The true impact of human disturbance on piedmonts cannot be understood without quantifying the baseline, long-term process rates that modify piedmont surfaces.

Piedmont morphology allows one to define qualitatively the dominant processes modifying the surface. *Simple* planar piedmonts may experience sheetfloods (McGee, 1897; Nichols *et al*., in review; Rahn, 1967; Schumm, 1962); some have uniformly active surfaces where all exposed sediment is transported down piedmont (Nichols *et al*., 2002). Alternatively, simple piedmonts may have shallow ephemeral channels that migrate laterally over the entire piedmont surface on sub-millennial time-scales (Nichols *et al*., 2002). *Complex* piedmonts have sediment that is transported in discrete ephemeral channels over only a small percentage of the surface area (Bull, 1991; Denny, 1967). Complex piedmonts have multiple surfaces of varying ages, and may have sediment erosion, deposition, and transport active at any one time in different places.

Most understanding of desert piedmont process rates comes either from direct measurement or modeling (Abrahams *et al*., 1988; Abrahams *et al*., 1991; Cooke, 1970; Cooke and Mason, 1973; Cooke and Reeves, 1972; Edinger-Marshall and Lund, 1999; Parsons and Abrahams, 1984; Rahn, 1967). Direct measurement of piedmont processes provides data for only a few years or decades (Laronne and Reid, 1993; Reid and Laronne, 1995; Schick *et al*., 1987). Such short-term data may not capture the geomorphically significant events that control long-term average process rates (Kirchner *et al*., 2001; Trimble, 1977). Measured rates are only representative of the time period over which the data were collected; extrapolation to longer-terms is uncertain (Kirchner *et al*., 2001). Alternatively, controlled models of simulated rainfall on desert piedmonts or in flumes (Abrahams *et al*., 1988; Luk *et al*., 1993) can replicate

changing climatic regimes. However, simulation models only quantify process rates for small, uniform areas (m^2). Scaling experimental results to an entire piedmont is also uncertain.

Long-term rates of piedmont processes are difficult to quantify because sediment transport, deposition, and erosion processes are affected by changing climates and piedmont morphologies (Baker and Twidale, 1991; Bull, 1991). Soil development is a powerful qualitative tool for investigating the long-term behavior of piedmonts because soil genesis depends on climate and time (Birkeland, 1984; McFadden *et al*., 1989; Wells *et al*., 1987). However, since soil development also depends on several difficult-to-measure regional variables, including carbonate influx and microclimate (Birkeland, 1984), soil data provide at best relative piedmont histories.

Recently, application of cosmogenic nuclides and mathematical models, set in a context using soil development, has extended our knowledge of piedmont behavior by quantifying long-term process rates that modify both simple and complex piedmonts (Nichols *et al*., in review; Nichols *et al*., 2002; Phillips *et al*., 1998; Pohl, 1995). Such studies demonstrate that piedmont process rates, including average downslope sediment velocities (decimeters per year), sediment deposition rates (mm ky^{-1}), and the timing of depositional hiatuses (process transition), are similar regardless of the complexity of piedmont surfaces (Nichols *et al*., in review).

We chose to investigate a multi-surface, disturbance-impacted piedmont in the Mojave Desert, at the Ft. Irwin army facility (Fig. 1). Measuring cosmogenic nuclides in samples collected over this wide (3 km) and long (6 km) piedmont allows us to quantify baseline piedmont processes over long time- and large spatial-scales. Our data provide the context in which to understand the affects of human disturbance on piedmont process rates.

GEOLOGIC SETTING

Fort Irwin (> 2,400 km^2) contains numerous desert piedmonts. We chose the *East Range Road* piedmont because it is backed by quartz-rich uplands and because it is wide and long (Fig. 1). Like most of the northern Mojave Desert, Fort Irwin has experienced extensive tectonic activity throughout the late Cenozoic (Sobieraj, 1994).

The uplands that supply sediment to the East Range Road piedmont consist of poorly indurated Tertiary alluvial fan deposits (mostly derived from granitic parent material) and have a maximum relief of ~ 300 m. The upland sediments conformably overlie a thick sequence (165 m) of lacustrine deposits, suggesting filling of a playa basin (Sobieraj, 1994). The lacustrine deposits are 11.65 my old (^{40}Ar-^{39}Ar date from Sandine crystals from an interbedded crystal-rich tuff) thus, providing a limiting age for overlying fan deposits and the East Range Road piedmont (Sobieraj, 1994). The piedmont is no older than late Miocene.

The East Range Road piedmont has two main surfaces. From the uplands, extending ~1.5 km down piedmont, there is a higher surface (incised < 4 m by ephemeral channels) which exhibits weak deserts pavements, with some varnished clasts (Fig. 2A). The presence of clasts of soil carbonate at the surface suggests that the upper piedmont is eroding. At ~1.5 km from the mountain front, the incised surface and the ephemeral channels merge to form a broad active surface (Fig. 2B). The surface lacks large clasts and it appears that all sediment was recently in transport. Most military activity happens on the low surface (Fig. 1). The average slope from the uplands to 6 km away is 1.9°. The piedmont drains to ephemeral Red Lake playa (~ 20 km away).

The East Range Road piedmont has been used periodically as an U.S. Army training range since 1940. In 1981, Ft. Irwin became a permanent training facility and the East Range

Road piedmont has experienced significant disturbance since then. Each month, wheeled and tracked vehicles (tanks) traverse the surface during training exercises destroying most of the vegetation and the shallow channels that drain the piedmont (Fig. 2B). Each runoff event establishes new ephemeral channels that are soon destroyed by the next round of training exercises.

The East Range Road piedmont is warm and dry. At Barstow, California, ~60 km south, average maximum temperature ranges from 15.4°C in December to 39°C in July and an average of 10.3 cm of rain falls annually (http://www.wrcc.dri.edu/cgi-bin/cliNORMtM.pl?cabars). Most of the precipitation comes either in short-duration intense summer cyclonic events or in long-duration, less intense frontal storms.

METHODS

East Range Road piedmont sediment is supplied by several narrow basins which cut into the upland Tertiary fan deposits (Fig. 1). In order to obtain the baseline nuclide activity of sediment exiting the uplands, we amalgamated sediment from three ephemeral channels that drain the upland source basins (Fig. 1). Nuclide activities measured in quartz extraed from this sediment allows us to determine source basin sediment generation rates (Bierman and Steig, 1996; Brown *et al*., 1995; Granger *et al*., 1996) and thus the flux of sediment onto the piedmont.

The piedmont surface that abuts the uplands is incised (< 4 m) by active ephemeral channels both connected to the drainages from the uplands and originating on the incised surface. These locally sourced channels erode and supply sediment to the through-going channels sourced in the uplands. In order to determine both the mass and cosmogenic nuclide contribution of the

incised surface, we amalgamated sediment from three channels that originate on and drain only the incised surface.

The sediment supplied to the piedmont is a mixture of sediment derived from the uplands (ERV-UB; Fig. 3) and sediment derived from erosion of the incised alluvial surface (ERV-P; Fig. 3). We collected a sediment sample at the distal end of the incised surface from the channels that originate in the uplands but also are fed by smaller channels arising on the incised surface. Since upland and incised surface sediments have different nuclide activities, we developed a simple two component mixing model to determine the percentage of sediment entering the piedmont from each source.

We amalgamated sediment along 3-km-long transects spaced 1-km intervals down the East Range Road piedmont to reflect the long-term average exposure of sediment that is transported down the wash surface (ERT-2 to ERT-6). Each transect sub-sample consisted of an equal volume of sediment mixed from 21 sampling locations spaced at 150 m intervals (piedmont transects). The piedmont transect samples are representative of the nuclide activity down the uniformly active lower piedmont surface.

We used a backhoe to open 2 pits (2.0 m and 1.4 m deep) on the East Range Road piedmont (Figs. 1 and 2). One pit was located on the incised surface close to the uplands (1.5 km); the other was located on the uniformly active surface near the middle of the piedmont (4 km from the uplands). We noted soil color, stratigraphy, grain size, texture, consistence, and soil horizonation (Table 1). On the basis of soil stratigraphy and soil horizonation, we divided each pit into depth intervals to sample for cosmogenic nuclide analysis. Each interval was continuous, so that the entire soil column exposed in each pit was analyzed.

Due to numerous unexploded ordinance on the East Range Road piedmont, we did not dig additional shallow soil pits to understand better the thickness of sediment that is in active transport, termed the *active transport layer (ATL)*. Such thicknesses are usually determined from the depth to the B horizon (Lekach *et al*., 1998; Nichols *et al*., 2002). In the few soil pits that we dug at East Range Road piedmont, the depth to the B-horizon is a few decimeters. We assume that the thickness of the ATL on the East Range Road piedmont is not significantly different than the thickness of the ATL on several other Mojave Desert piedmonts, a few decimeters (Nichols *et al*., in review; Nichols *et al*., 2002).

Samples were processed using accepted methods (Bierman and Caffee, 2001; Kohl and Nishiizumi, 1992). We analyzed quartz in the 500 to 850 μm size fraction to minimize the possibility of analyzing aeolian sediment. We did not analyze different grain sizes because previous grain size analyses demonstrate that all sediment grain sizes in arid regions have statistically similar nuclide activities (Clapp *et al*., 2002; Clapp *et al*., 2001; Clapp *et al*., 2000; Granger *et al*., 1996). Therefore, we assume that the 500 to 850 μm size-fraction represents all fluvially transported material. Accelerator mass spectrometry (AMS) analysis, at Lawrence Livermore National Laboratory, determined the $^{10}Be/^{9}Be$ and $^{26}Al/^{27}Al$ ratios. All measurements were blank corrected. In order to model the East Range Road data we use nominal production rates (sea level and > 60° latitude) of 5.2 ^{10}Be atoms g^{-1} and 30.4 ^{26}Al atoms g^{-1} (Bierman *et al*., 1996; Gosse and Phillips, 2001; Stone, 2000). We scaled the nominal production rates to the East Range Road altitude and latitude using no muons (Lal, 1991).

In order to quantify piedmont histories and processes, we use mathematical models to translate the nuclide activities into ages and rates. East Range Road piedmont surface processes rates operate on time scales much shorter than the nuclide half-lives (^{10}Be = 1.5 myr, ^{26}Al = 0.7

myr) therefore, surface processes control the nuclide activities, not radioactive decay. Since the uplands are dominantly quartz-rich Tertiary fan deposits, we assume no quartz enrichment through preferential dissolution of other minerals at East Range Road (Small *et al*., 1999).

We use previously published models of nuclide activity in sediment to estimate long-term basin erosion and sediment generation rates (Brown *et al*., 1995; Clapp *et al*., 2002; Clapp *et al*., 2000; Granger *et al*., 1996), to determine the near surface history of the piedmont, to quantify surface stability (Anderson *et al*., 1996), to quantify deposition rates (Lal and Arnold, 1985; Nichols *et al*., 2002; Phillips *et al*., 1998), and to determine the duration of depositional hiatuses (either erosion or surface of transport; Nichols *et al*., 2002). Sediment transport models use a mass and nuclide balance approach to translate the piedmont nuclide activities into long-term average sediment transport velocities (Nichols *et al*., 2002).

RESULTS

Sediment sources for the East Range Road piedmont are the upland basins and the eroding proximal piedmont. Regression of the ^{26}Al and ^{10}Be data indicate a ratio of 6.03 suggesting that the sediment samples have simple exposure histories (Fig. 4; Nishiizumi *et al*., 1989). Measurement precision averages 3% for ^{10}Be and 5% for ^{26}Al, therefore we base our models on ^{10}Be data because they are the more precisely measured.

The upper basin samples have the lowest average nuclide activity of all samples ($4.59 \pm 0.15 \times 10^5$ ^{10}Be atoms g^{-1}; Fig. 5), suggesting the shortest surface exposure history. The basins that drain only the incised alluvial surface (the eroding section of the piedmont) have higher average nuclide activities than the upland basins ($6.30 \pm 0.17 \times 10^5$ ^{10}Be atoms g^{-1}; Fig. 5), suggesting longer exposure histories than the upland sediment. The amalgamated sample that

consists of mixed upland basin sediment and incised alluvial surface sediment has an intermediate nuclide activity ($5.02 \pm 0.14 \times 10^5$ ^{10}Be atoms g^{-1}; ERV-LB in Fig. 5), consistent with the mixing of more-dosed sediment from the proximal piedmont and the less-dosed sediment from the upland basins.

Nuclide depth profiles for the two soil pits on the East Range Road piedmont have distinctively different shapes. EP1 has nuclide activities that generally decrease with depth (Fig. 6). EP2 has nuclide activities that neither increase nor decrease at depth (Fig. 7). The top-most three samples of EP1, which is closer to the uplands and up gradient of EP2, have higher nuclide activities than the all samples from EP2.

The nuclide activities for the piedmont transects increase in a nearly linear fashion from 0.77×10^6 ^{10}Be atoms g^{-1} at ERT-2 to 1.02×10^6 ^{10}Be atoms g^{-1} at ERT-6 (Fig. 5). These nuclide activities support the field observation that the source of transect sediment is a mixture of upland basin sediment (0.46×10^6 ^{10}Be atoms g^{-1}) and proximal piedmont sediment (0.85 to 0.96×10^6 ^{10}Be atoms g^{-1}). The steady increase in nuclide activity down the piedmont suggests regular dosing of sediment in transport.

DISCUSSION

Nuclide data allow insight into the long-term behavior of the East Range Road piedmont. Mathematical models translate nuclide activities into sediment generation rates, sediment velocities, sediment deposition rates, and the age of the incised alluvial surface (Nichols et al., 2002). By understanding the style, distribution, and rates of processes active on the East Range Road piedmont, we can better place contemporary human impact in the context of baseline piedmont behavior.

Sediment generation rates of upland basins and the eroding piedmont.

Sediment is generated from the uplands and from the eroding proximal piedmont. Using the sediment generation models, the average basin-wide lowering rate (average of ^{10}Be and ^{26}Al data) is 13 ± 3 mm ky^{-1} equivalent to a sediment flux from the upland basins to the piedmont of 3.62 x 10^4 kg y^{-1} km^{-2}. These rates are low compared to other basin-wide erosion rates in arid regions. The Iron and Granite Mountains in the southern Mojave Desert are lowering at 31 to 33 mm ky^{-1} (Nichols *et al*., 2002). The Chemehuevi Mountains in the eastern Mojave Desert are lowering at 41 mm ky^{-1} (Nichols *et al*., in review; Nichols *et al*., 2002). The granitic Fort Sage Mountains are lowering at 30 to 60 mm ky^{-1} (Granger *et al*., 1996). Perhaps the low basin-scale erosion rates (and the low basin sediment yields to the East Range Road piedmont) may be, in part, due to the greater infiltration capacity, and thus low runoff yield, of Tertiary alluvial fan deposits compared to crystalline bedrock.

The eroding proximal piedmont supplies additional sediment to the distal piedmont surface. Assuming a weighted average mixing model, the uplands supply 75% of sediment to the distal piedmont and the more highly-dosed, incised proximal piedmont supplies 25% of the sediment (Fig. 3). The proximal piedmont supplies an additional 1.31 x 10^4 kg y^{-1} km^{-2} to the down piedmont sediment flux complementing the 3.62 x 10^4 kg y^{-1} km^{-2} supplied by the upland basins.

Soil pit interpretive models

Incised alluvial surface pit (EP1). Nuclide activity in the soil pit located on the proximal incised alluvial surface (EP1) decreases as a function of depth, suggesting rapid deposition followed by stability. Averaging the ^{10}Be and ^{26}Al data, we calculate that the upper surface is at least 76,000 years old (Fig. 6; Anderson *et al*., 1996). This is a minimum limiting age because

soil carbonate, exposed on the incised surface suggests erosion. The calculated nuclide activity at the time of deposition of the sediment exposed today in EP1 was 4.5 x 10^5 atoms g^{-1}, similar to the nuclide activity of sediment currently issuing from the upland basins (4.6 ± 0.1 x 10^5 atoms g^{-1}). Such consistency in nuclide activity suggests that source basin erosion rates have been similar over at least the past 76,000 years. The ≥ 76,000 yr age of the eroding piedmont is reasonable considering the soil development in the pit and the K-horizon (stage III) at the bottom of the pit (Birkeland, 1984).

Wash surface pit (EP2). Three distinct buried soil horizons in EP2 (43 cm, 84 cm, and 118 cm) represent times of surface stability on the distal piedmont; however, nuclide activities neither increase nor decrease with depth in this pit as would be expected if there were extended periods of stability and soil formation (Fig. 7). The simplest interpretation of the nuclide data suggests recent and rapid deposition of all of the sediment to a depth of 118 cm. However, a stage III K-horizon at the bottom of the soil pit, and the intensity of soil development throughout the pit argue against recent, rapid deposition. There are depositional scenarios consistent with both the soil and nuclide data. Such scenarios require that the nuclide activities of the deposited sediment change over time. We constrain inherited nuclide activities within limits set by upland basin sediment (4.6 ± 0.15 x 10^5 atoms g^{-1}) and by the present nuclide activity of the soil pit surface sediment (8.5 ± 0.25 x 10^5 atoms g^{-1}).

Using the mathematical model of Nichols *et al*. (2002), we quantify deposition rates and durations of stability at pit EP1. The period of stability for each buried soil is modeled between 7,000 and 10,000 years at 118 cm, 15,000 to 25,000 years at 84 cm, and 20,000 years at 43 cm (Fig. 7). Deposition rates range from 40 to 150 mm ky^{-1} between 118 and 84 cm, 80 to 100 mm ky^{-1} between 84 to 43 cm, and 250 mm ky^{-1} from 43 cm to the surface. The total time represented

by these scenarios is between 57,000 to 75,000 years. Such soil pit ages are sufficient to develop the observed soils (Fig. 7).

The top 43 cm of EP1 can also be interpreted as young soil (< 2,000 years). The average nuclide activity of the top most 43 cm ($8.46 \pm 0.25 \times 10^5$ atoms g^{-1}; Fig. 7) is similar to the average nuclide activity of sediment in transport down the piedmont (8.33×10^5 atoms g^{-1}; Fig. 5) at the location (4 km) of the soil pit. Since nuclide activities of sediment in transport and of sediment in the uppermost strata of the soil pit are similar, and since soil development is weak, the top 43 cm of sediment is likely sediment in active transport down the piedmont with a residence time of < 2000 years at this location.

Comparison of EP1 and EP2 and regional climate. The two soil pits are consistent with similar piedmont histories. More than 76,000 years ago, a large volume of sediment was delivered to the entire piedmont. Such sediment deposition is consistent with a more moisture effective climate and pluvial lake level rises in and near Death Valley 80,000 yr ago (Reheis *et al*., 1996). Subsequently, a change to a drier climate reduced vegetation and increased stream power, which eroded the source basins and the more highly dosed proximal piedmont sediment and deposited it on the distal piedmont. Lake Manley in Death Valley had another highstand ~30,000 yr. ago (Lowenstein *et al*., 1994) which is consistent with deposition on the distal piedmont (EP2; 84 cm to 43 cm) at that time.

Sediment transport velocities. We quantify the sediment velocity down the East Range Road piedmont using a mass and nuclide balance model (Nichols *et al*., 2002). Using the parameters we measured at the East Range Road piedmont, the nuclide and mass balance model fits the data well (Fig. 8). The model suggests that present-rates of substrate erosion range from 1 mm ky^{-1} near the mountain front to 5 mm ky^{-1}, 6 km down piedmont. The average grain speed

down the Chemehuevi Mountain piedmont increases from 8 cm y^{-1} from the mountain front to 23 cm y^{-1} at the last transect, 6 km down gradient. The total transit time for sediment across the East Range Road piedmont is ~48,000 years.

EAST RANGE ROAD PIEDMONT AND OTHER MOJAVE DESERT PIEDMONTS

The East Range Road piedmont has process rates similar to several other Mojave Desert piedmonts (Nichols *et al*., in review; Nichols *et al*., 2002). Average sediment transport speeds down the complex East Range Road piedmont, the complex Chemehuevi Mountain piedmont, and the simple Iron and Granite Mountain piedmonts all average decimeters per year (Nichols *et al*., in review; Nichols *et al*., 2002). Similar average mobile sediment speeds on such different surfaces suggest that long-term sediment transport does not depend on piedmont morphology.

Piedmont depositional histories correlate poorly (Fig. 9). Lack of correlation could be due to differing source basin sensitivity to climate change. Where uplands erode more quickly (Iron and Chemehuevi Mountains; Nichols *et al*., in review; Nichols *et al*., 2002), sediment supply is large enough to allow uniform net deposition on distal piedmonts until the Pleistocene-Holocene climate change (~ 10 kyr ago), when there is a change in behavior to sediment transport. Where uplands erode slowly (East Range Road) sediment supply is low enough that deposition is not uniform and piedmont-wide (Fig. 9). Such depositional gaps create stable surfaces and allow soil development (EP2).

On complex piedmonts, Chemehuevi Mountain (Nichols et al., in review) and East Range Road, proximal surfaces do not have similar morphologies, ages, or periods of erosion (Fig. 9). Such differences in proximal piedmont process could be due to sediment flux from the uplands (climate perturbations) not supplying enough sediment to resurface the proximal piedmont.

Alternatively, the channels incised into the proximal piedmont surface could be too deep to allow surface deposition.

ANTHROPOGENIC INFLUENCE ON LONG-TERM PIEDMONT PROCESSES

The cosmogenic nuclide technique that we employed suggests similar long-term average sediment velocities down the highly disturbed East Range Road piedmont, the undisturbed Chemehuevi Mountain piedmont (Nichols *et al*., in review), and the Iron and Granite Mountain piedmonts which were disturbed for only a short time during World War II (Nichols and Bierman, 2001; Nichols *et al*., 2002). These results suggest that measurements of long-term piedmont process rates are robust in spite of different land use and disturbance histories. Therefore, one can measure contemporary sediment velocities on disturbed piedmonts and compare them to baseline rates to understand the magnitude of disturbance.

At the East Range Road piedmont, the Army has disturbed the surface for over six decades. Short-term sediment movement rates, as determined from monitoring 400 surface pebbles over 23 months, average 34 cm y^{-1} (Persico et al., in review). During this 2 yr study, precipitation gauges surrounding the East Range Road piedmont did not record significant rainfall volumes or intensities. By allowing for large decadal or centennial storm events the increased precipitation will create more overland flow, more runoff, and larger discharges which will increase the average sediment movement rate. For comparison, long-term sediment movement rates estimated using cosmogenic nuclides, at the East Range Road piedmont are 8 to 23 cm y^{-1}. By comparing both contemporary and baseline rates of sediment movement, we learn that extensive Army disturbance has increased average near surface sediment movement rates up to four fold or greater. Although it is apparent that extensive disturbance by wheeled and tracked

vehicles has significantly altered the sediment movement rates on the East Range Road piedmont, the overall movement of sediment is slow. Extrapolation of the short-term movement rates over the next 100 yr suggests average movement of only 34 m. Such slow sediment transport rates suggest that environmental impacts on desert piedmonts are long lasting. The comparison of long-term background and short-term anthropogenic influenced sediment movement rates demonstrates the utility of implementing a multi-scaled approach to quantify the impact of man on natural systems.

ACKNOWLEDGEMENTS

We thank L. Persico for field assistance, R. Sparks and the ITAM crew for logistical support, A. Matmon and B. Copans for sample preparation assistance, and P. Fahnstock for excavating the soil pits. This research supported by DEPSCoR grant #DAAD199910143 to Bierman and the Jonathan O. Davis and J. Hoover Mackin scholarships to Nichols.

REFERENCES

Abrahams, A. D., Parsons, A. J., and Luk, S. H. (1988). Hydrologic and sediment responses to simulated rainfall on desert hillslopes in southern Arizona. *Catena* **15,** 103-117.

Abrahams, A. D., Parsons, A. J., and Luk, S. H. (1991). The effect of spatial variability in overland flow on the downslope pattern of soil loss on a semiarid hillslope, southern Arizona. *Catena* **18,** 239-254.

Anderson, R. S., Repka, J. L., and Dick, G. S. (1996). Explicit treatment of inheritance in dating depositional surfaces using in situ 10Be and 26Al. *Geology* **24,** 47-51.

Baker, V. R., and Twidale, C. R. (1991). The reenchantment of geomorphology. *Geomorphology* **4,** 73-100.

Bierman, P., Larson, P., Clapp, E., and Clark, D. (1996). Refining estimates of 10-Be and 26-Al production rates. *Radiocarbon* **38,** 149.

Bierman, P. R., and Caffee, M. W. (2001). Slow rates of rock surface erosion and sediment production across the Namib Desert and escarpment, Southern Africa. *In* "The steady-state orogen; concepts, field observations, and models American Journal of Science 301, no. 4-5 (200105)." (F. J. Pazzaglia, and P. L. K. Knuepfer, Eds.), pp. 326-358. Yale University, Kline Geology Laboratory, New Haven, CT.

Bierman, P. R., and Steig, E. J. (1996). Estimating rates of denudation using cosmogenic isotope abundances in sediment. *Earth surface processes and landforms* **21,** 125-139.

Birkeland, P. W. (1984). "Soils and geomorphology." Oxford University Press, New York.

Brown, E. T., Stallard, R. F., Larsen, M. C., Raisbeck, G. M., and Yiou, F. (1995). Denudation rates determined from the accumulation of in situ-produced 10Be in the Luquilo Experimental Forest, Puerto Rico. *Earth and Planetary Science Letters* **129,** 193-202.

Bull, W. B. (1991). "Geomorphic responses to climate change." Oxford University Press, New York.

Clapp, E. M., Bierman, P. R., and Caffee, M. (2002). Using ^{10}Be and ^{26}Al to determine sediment generation rates and identify sediment source areas in an arid region drainage. *Geomorphology* **45,** 89-104.

Clapp, E. M., Bierman, P. R., Nichols, K. K., Pavich, M., and Caffee, M. (2001). Rates of sediment supply to arroyos from upland erosion determined using *in situ*-produced cosmogenic 10Be and 26Al. *Quaternary Research* **55,** 235-245.

Clapp, E. M., Bierman, P. R., Schick, A. P., Lekach, J., Enzel, Y., and Caffee, M. (2000). Sediment yield exceeds sediment production in arid region drainage basins. *Geology (Boulder)* **28,** 995-998.

Cooke, R. U. (1970). Morphometric analysis of pediments and associated landforms in the western Mojave Desert, California. *American Journal of Science* **269,** 26-38.

Cooke, R. U., and Mason, P. F. (1973). Desert Knolls Pediment and associated landforms in the Mojave Desert, California. *Revue de geomorphologie dynamique* **22,** 49-60.

Cooke, R. U., and Reeves, R. W. (1972). Relations between debris size and the slope of mountain fronts and pediments in the Mojave Desert, California. *Zeitschrift fur Geomorphologie* **16,** 76-82.

Denny, C. S. (1967). Fans and pediments. *American Journal of Science* **265,** 81-105.

Edinger-Marshall, S. B., and Lund, J. (1999). Gravel dispersion on a granite pediment (East Mojave Desert, California): A short-term look at erosional processes. *Earth Surface Processes and Landforms* **24,** 349-359.

Gosse, J. C., and Phillips, F. M. (2001). Terrestrial in situ cosmogenic nuclides: theory and application. *Quaternary Science Reviews* **20,** 1475-1560.

Granger, D. E., Kirchner, J. W., and Finkel, R. (1996). Spatially averaged long-term erosion rates measured from *in situ* produced cosmogenic nuclides in alluvial sediment. *The Journal of Geology* **104,** 249-257.

Iverson, R. M. (1980). Processes of accelerated pluvial erosion on desert hillslopes modified by vehicular traffic. *Earth Surface Processes* **5,** 369-388.

Iverson, R. M., Hinckley, B. S., Webb, R. M., and Hallet, B. (1981). Physical effects of vehicular disturbances on arid landscapes. *Nature* **212,** 915-917.

Kirchner, J. W., Finkel, R. C., Riebe, C. S., Granger, D. E., Clayton, J. L., King, J. G., and Megahan, W. F. (2001). Mountain erosion over 10 yr, 10 k.y., and 10 m.y. time scales. *Geology (Boulder)* **29,** 591-594.

Kohl, C. P., and Nishiizumi, K. (1992). Chemical isolation of quartz for measurement of *in situ*-produced cosmogenic nuclides. *Geochimica et Cosmochimica Acta* **56,** 3583-3587.

Lal, D. (1991). Cosmic ray labeling of erosion surfaces: *In situ* nuclide production rates and erosion models. *Earth and Planetary Science Letters* **104,** 424-439.

Lal, D., and Arnold, J. R. (1985). Tracing quartz through the environment. *Proceeding of the Indian Academy of Science* **94,** 1-5.

Laronne, J. B., and Reid, I. (1993). Very high rates of bedload sediment transport by ephemeral desert rivers. *Nature* **366,** 148-150.

Lekach, J., Amit, R., Grodek, T., and Schick, A. P. (1998). Fluvio-pedogenic processes in an ephemeral stream channel, Nahal Yael, Southern Negev, Israel. *Geomorphology* **23,** 353-369.

Lowenstein, T. K., Li, J., Brown, C. B., Spencer, J. F., Roberts, S. M., Yang, E., Ku, T. L., and Luo, S. (1994). Death Valley salt core: 200,000 year record of closed-basin subenvironments and climates. *Geological Society of America Abstracts with Programs* **26,** 169.

Luk, S.-h., Abrahams, A. D., and Parsons, A. J. (1993). Sediment sources and sediment transport by rill flow and interrill flow on a semi-arid piedmont slope, southern Arizona. *Catena* **20,** 93-111.

McFadden, L. D., Ritter, J. B., and Wells, S. G. (1989). Use of multiparameter relative-age methods for age estimation and correlation of alluvial fan surfaces on a desert piedmont, eastern Mojave Desert, California. *Quaternary Research* **32,** 276-290.

McGee, W. J. (1897). Sheetflood erosion. *Bulletin of the Geological Society of America* **8,** 87-112.

Nichols, K. K., and Bierman, P. R. (2001). Fifty-four years of ephemeral channel response to two years of intense military activity, Camp Iron Mountain, Mojave Desert, California. *In* "The environmental legacy of military operations." (R. Harmon, and J. Ehlen, Eds.), pp. 123-136. Geological Society of America, Boulder.

Nichols, K. K., Bierman, P. R., Eppes, M. C., Caffee, M., Finkel, R., and Larsen, J. (in review). Deciphering the Late Pleistocene and Holocene history of the complex Chemehuevi Mountain piedmont using ^{10}Be and ^{26}Al. *American Journal of Science*.

Nichols, K. K., Bierman, P. R., Hooke, R. L., Clapp, E. M., and Caffee, M. (2002). Quantifying sediment transport on desert piedmonts using ^{10}Be and ^{26}Al. *Geomorphology* **45,** 105-125.

Nishiizumi, K., Winterer, E. L., Kohl, C. P., Klein, J., Middleton, R., Lal, D., and Arnold, J. R. (1989). Cosmic ray production rates of ^{10}Be and ^{26}Al in quartz from glacially polished rocks. *Journal of Geophysical Research* **94,** 17,907-17,915.

O'Hara, S. L. (1997). Human impacts on dryland geomorphic processes. *In* "Arid Zone Geomorphology: Process, Form and Change in Drylands." (D. S. G. Thomas, Ed.), pp. 639-658. John Wiley & Sons Ltd., London.

Parsons, A. J., and Abrahams, A. D. (1984). Mountain mass denudation and piedmont formation in the Mojave and Sonoran Deserts. *American Journal of Science* **284,** 255-271.

Persico, L. (2002). "Tracking painted pebbles on a Mojave Desert piedmont: Annual rates of sediment movement and the impact of off-road vehicles." Unpublished B.S thesis, University of Vermont.

Persico, L., Nichols, K. K., and Bierman, P. R. (2001). Tracking painted pebbles in the Mojave-Offroad vehicles and their impact on sediment transport. *Geological Society of America Abstracts with Programs* **33,** A-439.

Phillips, W. M., McDonald, E. V., Reneau, S. L., and Poths, J. (1998). Dating soils and alluvium with cosmogenic 21Ne depth profiles: case studies from the Pajarito Plateau, New Mexico, USA. *Earth and Planetary Science Letters* **160,** 209-223.

Pohl, M. M. (1995). Radiocarbon ages on organics from piedmont alluvium, Ajo Mountains, Arizona. *Physical Geography* **16,** 339-353.

Prose, D. V. (1985). Persisting effects of armored military maneuvers on some soils of the Mojave Desert. *Environmental Geology Water Science* **7,** 163-170.

Rahn, P. H. (1967). Sheetfloods, streamfloods, and the formation of pediments. *Annals of the Association of American Geographers* **57,** 593-604.

Reheis, M. C., Slate, J. L., Throckmorton, C. K., McGeehin, J. P., Sarna-Wojcicki, A. M., and Dengler, L. (1996). Late Quaternary sedimentation on the Leidy Creek fan, Nevada-California: geomorphic responses to climate change. *Basin Research* **12,** 279-299.

Reid, I., and Laronne, J. B. (1995). Bed load sediment transport in an ephemeral stream and a comparison with seasonal and perennial counterparts. *Water Resources Research* **31,** 773-781.

Schick, A. P., Lekach, J., and Hassan, M. A. (1987). Vertical exchange of coarse bedload in desert streams. *In* "Desert sediments: ancient and modern." (L. Frostick, and I. Reid, Eds.), pp. 7-16. Geological Society Special Publication, London.

Schumm, S. A. (1962). Erosion of miniature pediments in Badlands National Monument, South Dakota. *Geological Society of America Bulletin* **73,** 719-724.

Small, E. E., Anderson, R. S., and Hancock, G. S. (1999). Estimates of the rate of regolith production using ^{10}Be and ^{26}Al from an alpine hillslope. *Geomorphology* **27,** 131-150.

Sobieraj, J. A. (1994). "Sedimentology and tectonics of the tertiary fan deposits, Fort Irwin, northern Mojave Desert, California." Unpublished M.S. thesis, Western Washington University.

Stone, J. (2000). Air pressure and cosmogenic isotope production. *Journal of Geophysical Research* **105,** 23753-23759.

Thomas, D. S. G. (1997). Arid environments: their nature and extent. *In* "Arid Zone Geomorphology: Process, Form and Change in Drylands." (D. S. G. Thomas, Ed.), pp. 3-12. John Wiley & Sons Ltd., London.

Trimble, S. W. (1977). The fallacy of stream equilibrium in contemporary denudation studies. *American Journal of Science* **277,** 876-887.

Wells, S. G., McFadden, L. D., and Dohrenwend, J. C. (1987). Influence of Late Quaternary climatic changes on geomorphic and pedogenic processes on a desert piedmont, eastern Mojave Desert, California. *Quaternary Research* **27,** 130-146.

FIGURE CAPTIONS

Figure 1. Aerial photograph of the East Range Road piedmont. The upland/piedmont border is represented by dashed line. The upland basin sample (ERV-UB) is an amalgamation of sediment collected from the locations of the three black dots. Source basins are outlined in thin black lines. Thick black lines spaced at 1 km intervals represented transect locations (3 km long; ERT designation). Black boxes represent soil pit locations (EP1 and EP2). The eroding proximal piedmont sample (ERV-P) is an amalgamation of sediment collected from channels draining only incised alluvial surface (white dots). The sample that contains sediment sourced from both the source basins and the eroding piedmont (ERV-LB) is represented by the gray dots. White lines on piedmonts are roads used by tanks and wheeled vehicles.

Figure 2. Photographs of the East Range Road surface. A. Backhoe is on incised proximal piedmont surface. Foreground of photograph shows active channel. B. Photograph of wash surface on the East Range Road piedmont. The numerous tank tracks have destroyed the piedmont drainage network.

Figure 3. Sediment budget for East Range Road piedmont. Uplands (ERV-UB) supply 75% of sediment to distal piedmont while the eroding piedmont (ERV-P) supplies 25%. The percentage of upland and piedmont sourced sediment is calculated from the average nuclide activity of the mixed sediment entering the distal piedmont (EV-LB).

Figure 4. Regression of the ^{10}Be and the ^{26}Al data. The regression trendline of entire data set has a slope similar to the nominal production ^{10}Be/^{26}Al ratio of 6.0 indicating no significant burial during or after exposure and no nuclide inheritance from Tertiary source basin rocks.

Figure 5. Graph of nuclide activity down the piedmont for ^{10}Be data (A) and ^{26}Al data (B). Solid black squares represent transect data. Open square represents amalgamated sample characterizing incised alluvial surface sediment and ephemeral channel sediment (ERT-1). Open circle represents upland sediment datum (ERV-UB). Gray circle represents eroding piedmont datum (ERV-P). Black circle represents sediment mixture of ephemeral channel sediment and sediment eroded from piedmont (ERV-LB).

Figure 6. ^{10}Be data (A) and ^{26}Al data (B) for EP1. Data points represent mid-point of depth interval. Error bars represent 1σ analytical uncertainty. Black lines show model fit of 76,000 yrs. of surface stability.

Figure 7. ^{10}Be data (A) and ^{26}Al data (B) for EP2. Nuclide activity neither increases nor decreases with depth. Data points represent mid-point of depth interval. Black lines show model fit. Dashed lines represent buried soil horizons. Error bars represent 1σ analytical uncertainty.

Figure 8. Best fit of nuclide mixing model to the ^{10}Be data. Black line represents the model; the squares represent the ^{10}Be data. 1σ analytical error bars are smaller than the symbols. RMS error of the model is 38,000 atoms.

Figure 9. Depositional histories for proximal (P) and distal (D) soil pits on Iron Mountain (IM), Chemehuevi Mountain (CM), and East Range Road (ER) piedmonts. IM has simple surface morphology. CM and ERR have complex surface morphologies.

TABLE 1

Soil Pit Descriptions for the East Range Road Piedmont

Pit	Horizon[a]	Depth	Color[b]		Texture[c]	Structure[d]	Carbonate[e]
		(cm)	Moist	Dry			(%)
EP1	Av	0-6	10YR 4/4	10YR 6/3	L	3 c pl	
	Bw	6-16	7.5YR 4/4	10YR 5/4	L	f/m sbk	ef
	Bt	16-44	7.5YR 4/6	7.5YR 5/4	SL	2 m/c sbk	
	Btk	44-59	7.5YR 5/6	7.5YR 5/4	L	2 f/m sbk	stage II
	Btk2	59-77	7.5YR 4/4	7.5YR 5/4	SL	1 f sbk	stage I
	1Ck	77-100	7.5YR 4/4	10YR 6/4	LS	0.5 vf sbk	
	2Ck/K	100-210					
	Ck2		10YR 4/4	10YR 6/3	LS	sg	
	K		10YR 5/4	10YR 7/3	LS	m	stage III
EP2	A	0-5	10YR 4/3	10YR 6/4	LS	sg	
	Av	5-11	10YR 4/3	10YR 6/4	LS	2 m sbk	
	Bw	11-29	10YR 4/4	10YR 6/3	LS	2 m/c sbk	
	Ck	29-43	10YR 4/4	10YR 6/4	LS	1 f sbk	
	2Bkmb	43-60	7.5YR 5/4	10YR 6/5	LS	2 vf sbk	
	2Ck	60-84	10YR 5/4	10YR 6/5	LS	1 f sbk	
	Btbk	84-106	10YR 5/4	10YR 6/5	LS	2 m sbk	
	3Ck	106-118	10YR 5/4	10YR 6/4	LS	1 vf sbk	
	K	118-140	10YR 5/4	10YR 7/3	LS	m	stage III

TABLE 1 CONTINUTED

[a]Numbers preceding the horizon designation represent the following, for CP1 1= gravelly sand, 2 = sandy gravel, for EP2 overall coarsening down sequence from 1 to 3; [b]Color determined using Munsel color charts; [c]Textures are defined as L = loam, SL = sandy loam, and LS = loamy sand; [d]Structure defined as c = coarse, pl = platy, f = fine, m = medium, sbk = sub-angular blocky, vf = very fine, sg = sand and gravel; [e]Carbonate development defined as ef = effervesces with dilute HCl.

Nichols et al. Table 1

TABLE 2

Cosmogenic Nuclide Data for East Range Road Piedmont

Sample[1]	Elevation[2] (m)	Northing[3] (UTM)	Easting[3] (UTM)	^{10}Be activity[4] (10^6 atoms g^{-1})	^{26}Al activity[4] (10^6 atoms g^{-1})	^{26}Al/^{10}Be
ERV-UB	990	3918672	548155	0.459 ± 0.015	2.62 ± 0.146	5.78 ± 0.37
	1000	3918524	549577			
	930	3917713	550513			
ERV-LB	900	3917584	548022	0.502 ± 0.015	2.88 ± 0.136	5.73 ± 0.32
	840	3916421	549596			
	830	3916107	550302			
ERV-P	860	3916800	548269	0.630 ± 0.017	3.69 ± 0.172	5.86 ± 0.31
	830	3916069	549922			
	860	3916746	550367			
ERT-1	870	3917000	547800	0.587 ± 0.016	3.34 ± 0.155	5.68 ± 0.31
		3916750	550800			
ERT-2	810	3616000	547650	0.771 ± 0.021	3.93 ± 0.186	5.10 ± 0.28
		3915750	550650			
ERT-3	760	3915000	547500	0.802 ± 0.021	4.38 ± 0.204	5.47 ± 0.29
		3914750	550500			
ERT-4	720	3914000	547350	0.864 ± 0.028	4.78 ± 0.229	5.53 ± 0. 32
		3913750	550350			
ERT-5	695	3913000	547200	0.899 ± 0.024	4.95 ± 0.241	5.50 ± 0.30
		9312750	550200			

TABLE 2 CONTINUTED

ERT-6	680	3912200	547050	1.018 ± 0.035	5.78 ± 0.269	5.68 ± 0.33
		3911950	550050			
EP1 0-6	840	3916585	548869	0.850 ± 0.026	5.54 ± 0.289	6.51 ± 0.39
EP1 6-16				0.959 ± 0.028	5.49 ± 0.256	5.73 ± 0.31
EP1 16-30				0.877 ± 0.025	5.08 ± 0.256	5.79 ± 0.34
EP1 30-44				0.833 ± 0.022	4.69 ± 0.227	5.64 ± 0.31
EP1 44-59				0.773 ± 0.023	4.66 ± 0.217	6.03 ± 0.33
EP1 59-77				0.790 ± 0.023	5.08 ± 0.272	6.44 ± 0.39
EP1 77-90				0.719 ± 0.027	4.14 ± 0.202	5.75 ± 0.36
EP1 90-100				0.707 ± 0.018	4.07 ± 0.185	5.75 ± 0.30
EP1 100-125				0.726 ± 0.019	4.18 ± 0.190	5.76 ± 0.30
EP1 152-150				0.562 ± 0.016	3.49 ± 0.172	6.21 ± 0.35
EP1 150-175				0.566 ± 0.016	2.07 ± 0.102	3.65 ± 0.21
EP1 175-200				0.555 ± 0.016	3.25 ± 0.152	5.86 ± 0.32
EP2 0-11	755	3914895	549055	0.847 ± 0.023	5.00 ± 0.288	5.91 ± 0.38
EP2 11-29				0.856 ± 0.026	5.17 ± 0.248	6.03 ± 0.34
EP2 29-43				0.837 ± 0.023	5.18 ± 0.291	6.19 ± 0.39
EP2 43-60				0.835 ± 0.027	4.63 ± 0.219	5.55 ± 0.32
EP2 60-84				0.808 ± 0.022	4.19 ± 0.189	5.18 ± 0.28
EP2 84-95				0.808 ± 0.0 21	4.26 ± 0.204	5.27 ± 0.29
EP2 95-106				0.836 ± 0.023	4.88 ± 0.233	5.84 ± 0.32

TABLE 2 CONTINUTED

EP2 106-118	0.762 ± 0.021	4.12 ± 0.194	5.40 ± 0.30
EP2 118-140	0.815 ± 0.023	4.43 ± 0.234	5.44 ± 0.33

[1]Sample notation: ER = East Range Road, V = source basin sample, UB = upland basin, LB = mixture of upland sediment and eroding sediment, P = eroding piedmont sediment, UB, LB, and P each are an amalgamation of three samples, T = transect sample, EP1 represents proximal soil pit to the uplands, EP2 represents distal soil pit located ~4 km from uplands, numbers located after EP# represent depth intervals in centimeters. [2]All elevations are average upland valley elevation, based on basin hypsometry, and average elevation of the 3 km-long transects. [3]Northing and Easting values are NAD 27 zone 11S UTM datum. Coordinates are listed for all averaged valley samples. Endpoint coordinates are listed for transect samples. [4]Error is counting statistics from AMS with 2% uncertainty for stable Be and 4% uncertainty for stable Al, combined quadratically.

Nichols et al., Table 2

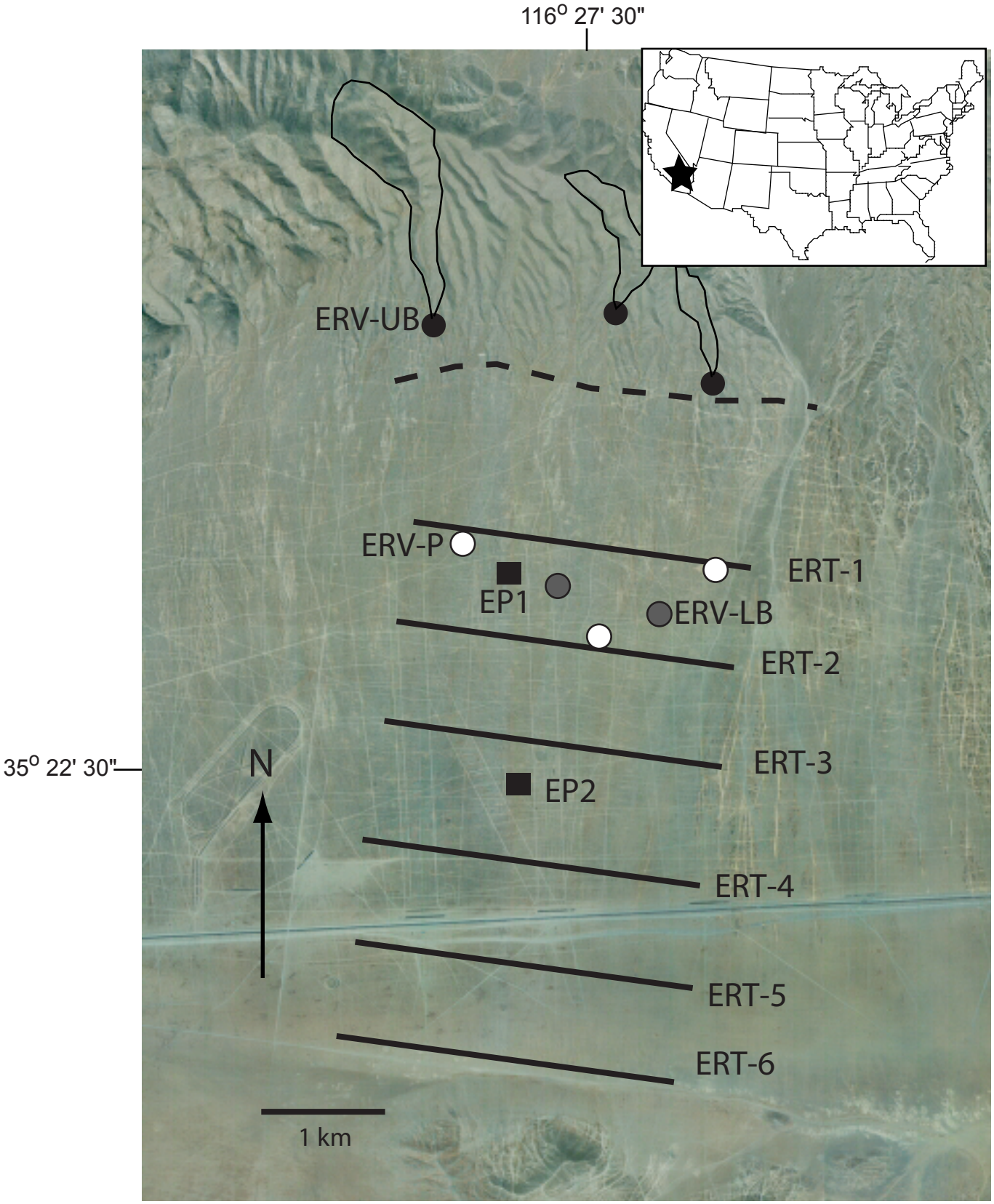

Nichols et al., Fig. 1

Nichols et al., Fig. 2

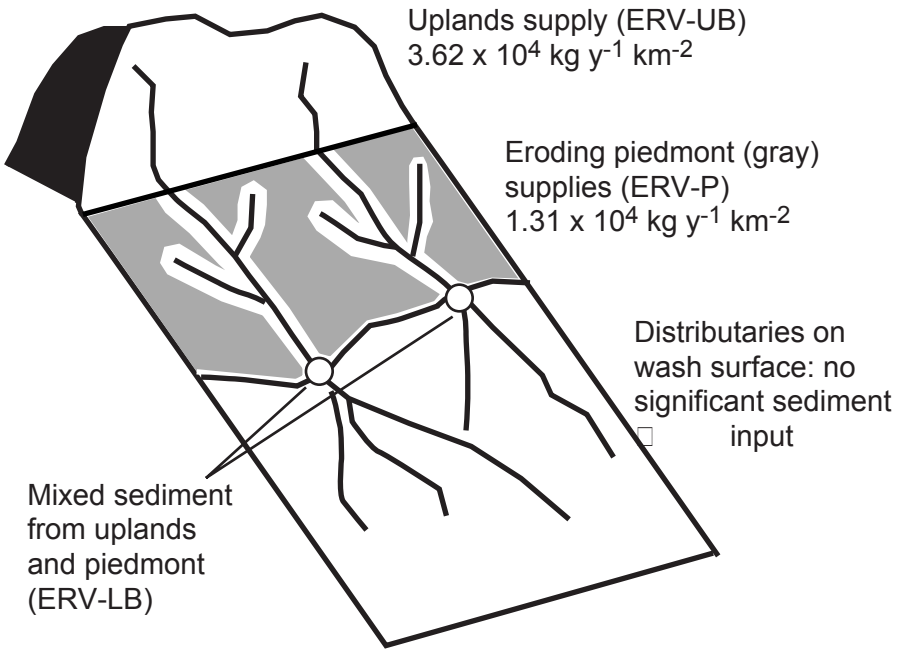

Nichols et al., Fig. 3

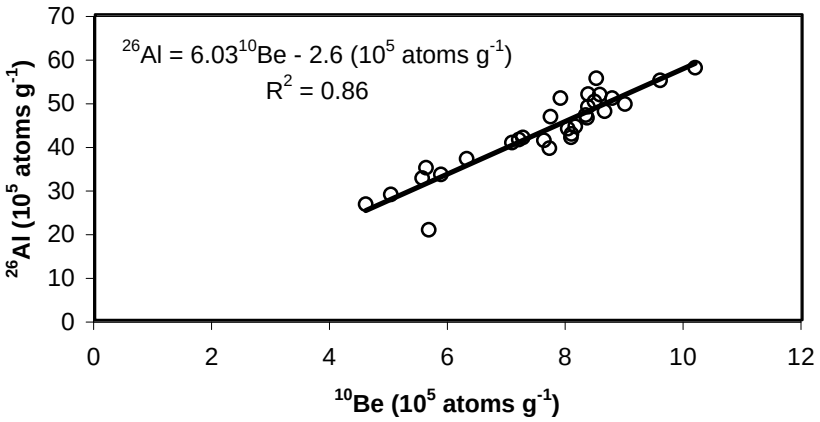

Nichols et al. Fig. 4

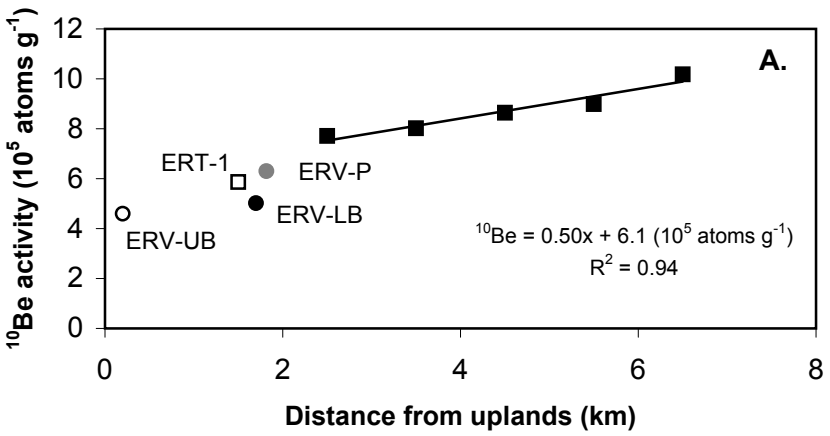

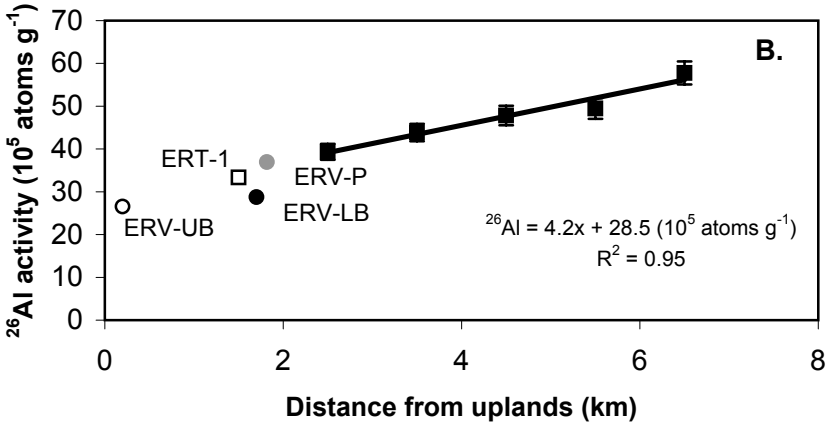

Nichols et al. Fig 5

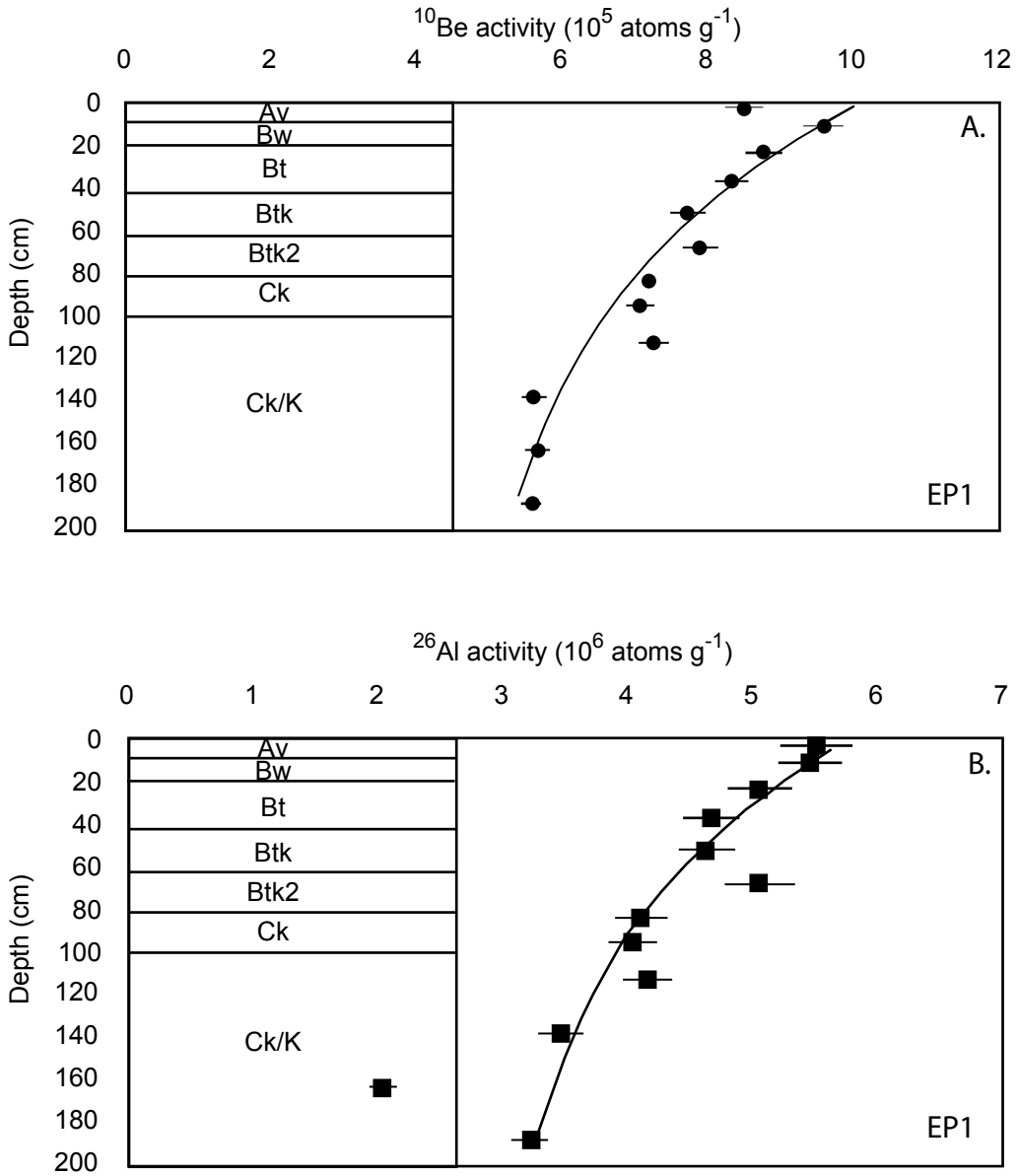

Nichols et al., Fig. 6

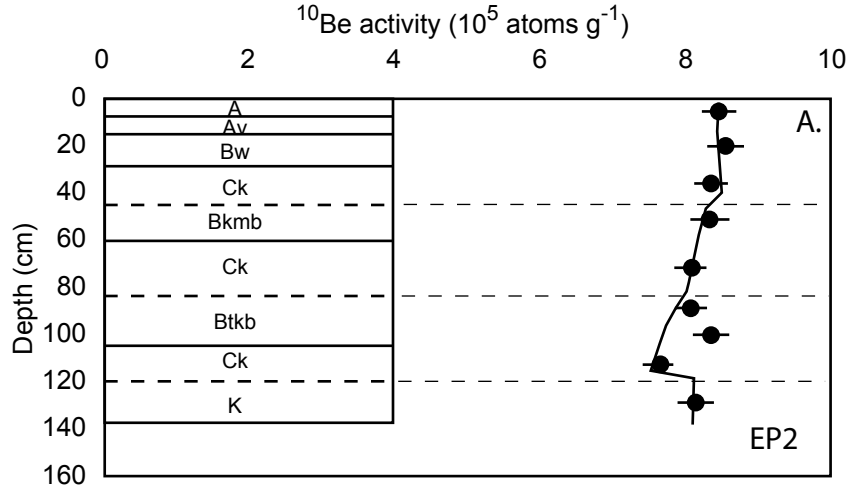

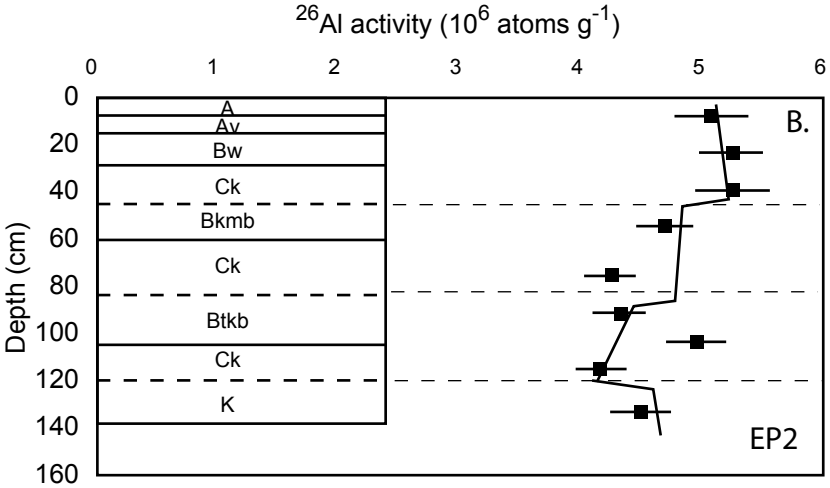

Nichols et al., Fig. 7

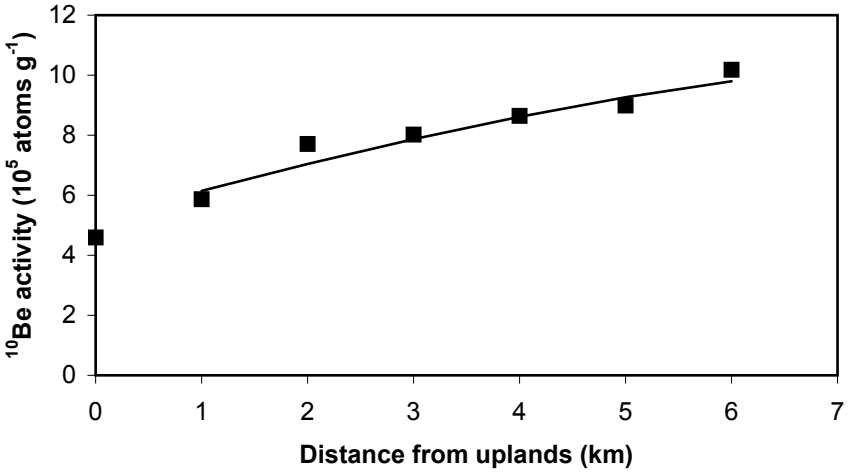
12
10
8
6
4
2
0
^{10}Be activity (10^5 atoms g^{-1})
0
1
2
3
4
5
6
7
Distance from uplands (km)

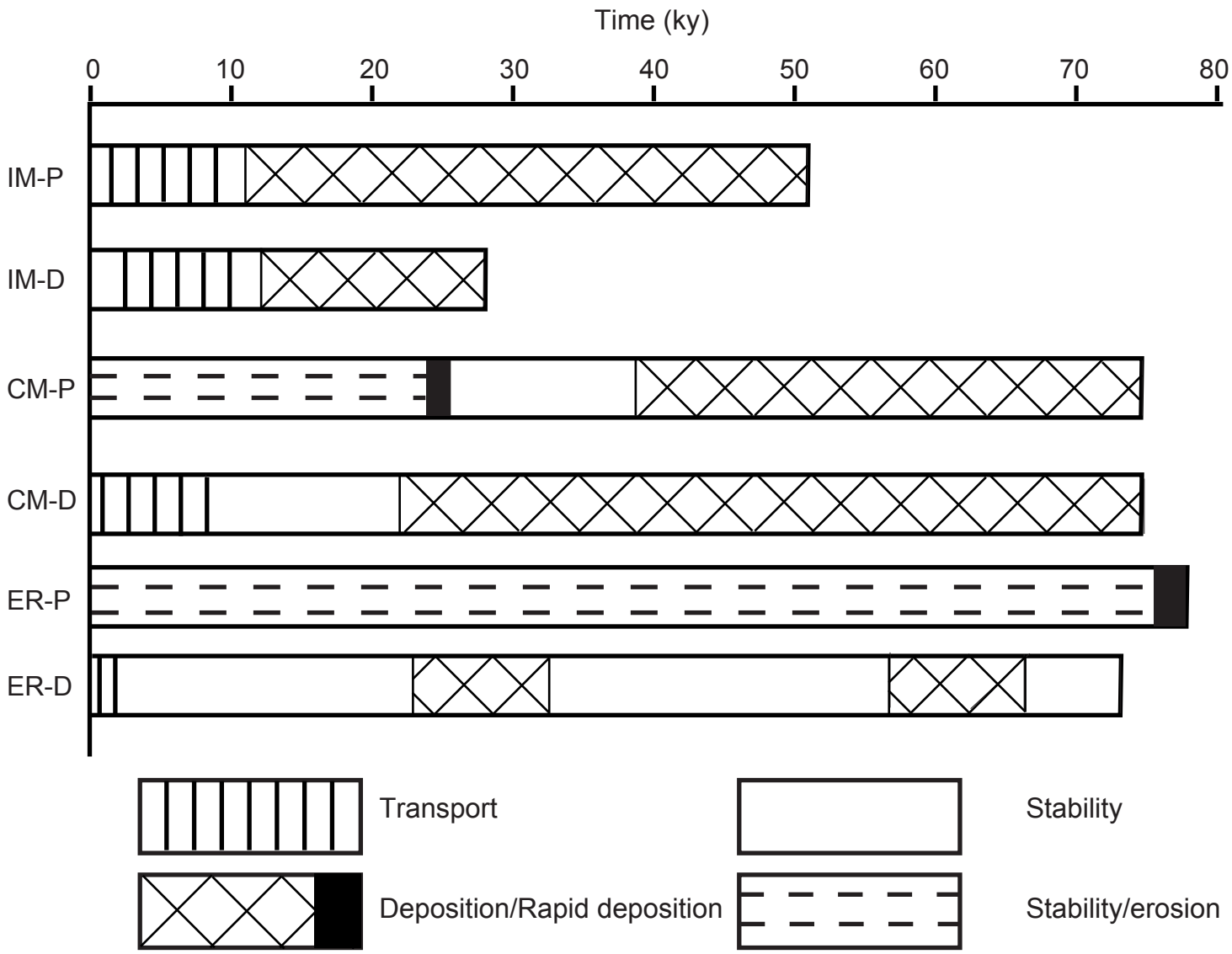

Nichols et al., Fig. 9